

# The Hidden Face of Wine Polyphenol Polymerization Highlighted by High-Resolution Mass Spectrometry

Anna Vallverdú-Queralt,<sup>\*[a]</sup> Emmanuelle Meudec,<sup>[a]</sup> Matthias Eder,<sup>[a]</sup> Rosa M. Lamuela-Raventos,<sup>[b, c]</sup> Nicolas Sommerer,<sup>[a]</sup> and Véronique Cheyner<sup>[a]</sup>

Polyphenols, including tannins and red anthocyanin pigments, are responsible for the color, taste, and beneficial health properties of plant-derived foods and beverages, especially in red wines. Known compounds represent only the emerged part of the “wine polyphenol iceberg”. It is believed that the immersed part results from complex cascades of reactions involving grape polyphenols and yeast metabolites. We used a non-targeted strategy based on high-resolution mass spectrometry and Kendrick mass defect plots to explore this hypothesis. Reactions of acetaldehyde, epicatechin, and malvidin-3-O-glucoside, representing yeast metabolites, tannins, and anthocyanins, respectively, were selected for a proof-of-concept experiment. A series of compounds including expected and so-far-unknown structures were detected. Random polymerization involving both the original substrates and intermediate products resulting from cascade reactions was demonstrated.

Polyphenols attract considerable interest because of their ubiquitous occurrence within the plant kingdom and their numerous important properties, related to their high structural diversity.<sup>[1]</sup> Owing to the acidic character of their hydroxyl groups and the nucleophilic properties of the phenolic rings, these molecules are highly reactive and undergo various types of reactions in the course of food processing and storage.<sup>[2]</sup> The major polyphenols in fruits and especially in grape are anthocyanins, the pigments of red and dark cultivars, and flavan-3-ols, including monomers (e.g. epicatechin) and proanthocyan-

din oligomers and polymers, commonly called tannins,<sup>[1,2]</sup> which confer astringency.<sup>[3]</sup> Their reactions, further increasing structural diversity, are responsible for the color and taste changes occurring during wine making and ageing, and may influence the health benefits of wine.<sup>[4]</sup> A number of reaction products have been unraveled in red wine.<sup>[5–7]</sup> In particular, oxygen exposure has been reported to promote the accumulation of products derived from reaction of anthocyanins and/or flavan-3-ols with acetaldehyde, a yeast metabolite and oxidation product of ethanol present in a large amount in wine.<sup>[8,9]</sup> Investigations in model solutions have shown that reactions of the red anthocyanin pigments with acetaldehyde yield both purple pigments<sup>[10]</sup> and orange pyranoanthocyanin derivatives.<sup>[11]</sup> However, known polyphenols, including tannins, red anthocyanin pigments, and reaction products identified so far, represent the emerged part of the “polyphenol iceberg”, explaining only a small proportion of the observed color. Similarly, oxidative browning of white wines is related to their flavan-3-ol content<sup>[12,13]</sup> and might result from flavan-3-ol reactions with acetaldehyde, but the structure of the brown pigments is still unknown. It is believed that the immersed part of the polyphenol iceberg results from random complex cascades of reactions involving grape polyphenols and other wine components such as yeast metabolites.

The purpose of the present work was to explore this hypothesis and shed light on the immersed part of the polyphenol iceberg. To this aim, non-targeted metabolomics approaches based on high-resolution mass spectrometry (HRMS) and petroleomics-derived data interpretation strategies, namely Kendrick mass defect plots, were implemented.<sup>[14]</sup> A simple model consisting of (–)-epicatechin (Ec) and malvidin-3-O-glucoside (Mv3G), representative of the two major families of grape polyphenols, and acetaldehyde, was selected to perform a proof-of-concept experiment. Using the restriction rules described in Supporting Information (Materials and Methods), 160 mass signals were retained and unambiguously attributed to elemental CHO compositions below 3 mmu tolerance.

In the selected model system, Ec and Mv3G are the two initial flavonoid building blocks. Mv3G exists as several forms in equilibrium.<sup>[13]</sup> In acidic aqueous solutions (pH < 2), the red flavylium cation (Mv3G<sub>F</sub>) is predominant. In mildly acidic solutions, such as wine, it undergoes nucleophilic attack of water at position 2 (or 4) of the pyrylium nucleus, leading to the colorless hemiketal (Mv3G<sub>OH</sub>), and deprotonation, giving rise to blue–purple quinonoid bases (Mv3G<sub>B</sub>).<sup>[15]</sup> This leads to four initial building blocks, as depicted in Figure 1.

Ec and Mv3G possess nucleophilic carbons in the 6 and 8 positions, which can react with protonated acetaldehyde to

[a] Dr. A. Vallverdú-Queralt, E. Meudec, M. Eder, Dr. N. Sommerer, Dr. V. Cheyner  
Department Sciences pour l'œnologie  
Institution INRA, UMR1083  
2 Place Pierre Viala, Montpellier 34000 (France)  
E-mail: avallverdu@ub.edu

[b] Dr. R. M. Lamuela-Raventos  
Nutrition and Food Science Department  
University of Barcelona  
Av Joan XXIII s/n, 08007 Barcelona (Spain)

[c] Dr. R. M. Lamuela-Raventos  
Instituto de Salud Carlos III, ISCIII (CIBEROBN)  
C/ Sinesio Delgado, 4, 28029 Madrid (Spain)

Supporting Information and the ORCID identification number(s) for the author(s) of this article can be found under <https://doi.org/10.1002/open.201700044>.

© 2017 The Authors. Published by Wiley-VCH Verlag GmbH & Co. KGaA. This is an open access article under the terms of the Creative Commons Attribution-NonCommercial-NoDerivs License, which permits use and distribution in any medium, provided the original work is properly cited, the use is non-commercial and no modifications or adaptations are made.

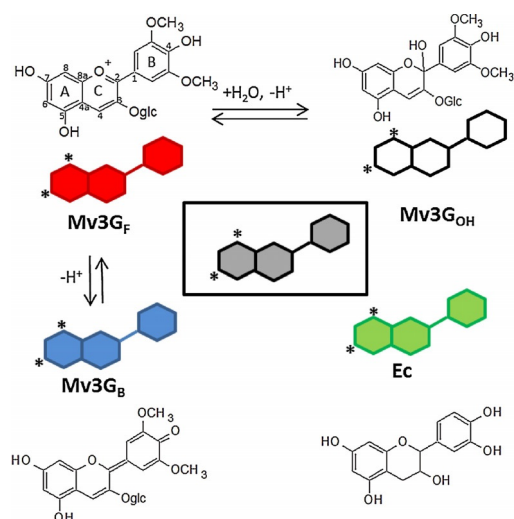


**Figure 1.** Initial building blocks of acetaldehyde mediated reaction. \*Nucleophilic activity.

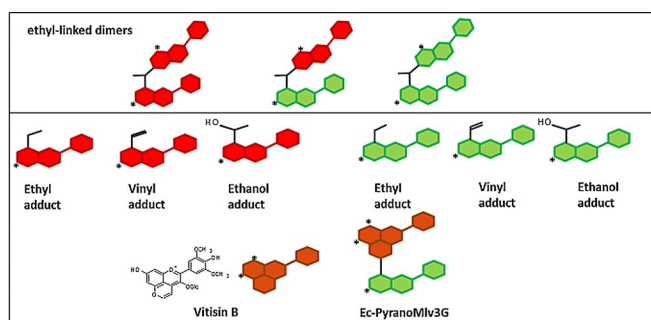


**Figure 2.** Other known building blocks arising from Mv3G<sub>F</sub> and Ec. \*Nucleophilic activity

yield ethanol–flavonoid adducts and methyl–methine-linked flavonoid dimers (called ethyl-linked dimers) (see Figure 2).<sup>[16,17]</sup> By dehydration and cleavage of the methyl-methine bridge, respectively, both generate vinyl-flavonoid intermediates and ethyl-flavonoids.<sup>[18]</sup> The flavylium cation can also undergo cycloaddition at the C-4 and 5-OH positions with vinylphenol structures<sup>[19]</sup> or with carbonyl compounds (with dehydration),<sup>[20]</sup> followed by an oxidation step to yield an additional pyrane ring. PyranoMv3G (vitisin B)<sup>[21]</sup> and Ec-pyranoMv3G,<sup>[22]</sup> resulting from reaction of Mv3G with acetaldehyde and with vinyl-Ec, respectively, have been detected in wine. All of these reaction products show nucleophilic activity in C-6 and C-8 positions and, thus, can be considered as additional building blocks for the acetaldehyde condensation (Figure 2).

To investigate step-growth condensation, a Kendrick plot was created with a mass increment corresponding to Ec-ethyl units (316 amu) based on the assumption that most compounds contained sequences of this structural motif. Each horizontal line corresponds to a series of compounds differing by the number of Ec-ethyl units, starting from a given base unit, as illustrated in Figure 3 for Ec and Mv3G.

Increases corresponding to Mv3G-ethyl units (518 amu) are also displayed, showing that Ec and Mv3G compete in random polymerization to yield a large number of Ec, Mv3G, and mixed Ec–Mv3G ethyl-bridged oligomers, containing up to 6, 4, and 10 units, respectively (Table S1, new compounds in bold). It should be emphasized that each signal detected represents several isomers with different random sequences and different linkage positions and conformations (6-6, 6-8, R and S, 8-8). Moreover, Mv3G was found in its different forms in the homogenous Mv3G polymers, as described earlier,<sup>[17]</sup> whereas the flavylium form was predominant in mixed derivatives, suggesting that they are less susceptible to hydration than Mv3G, as shown earlier for the dimers.<sup>[12]</sup> Note that the quinonoidal base form is detected as its protonated adduct and, thus, in

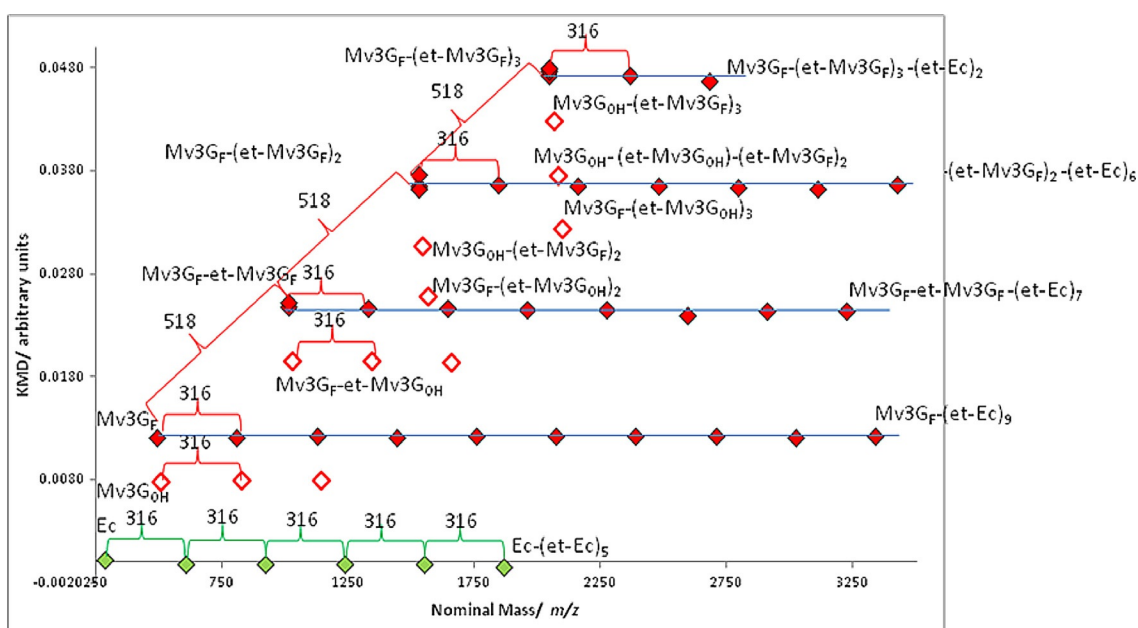


**Figure 3.** Diagram of Kendrick for Ec and Mv3G.

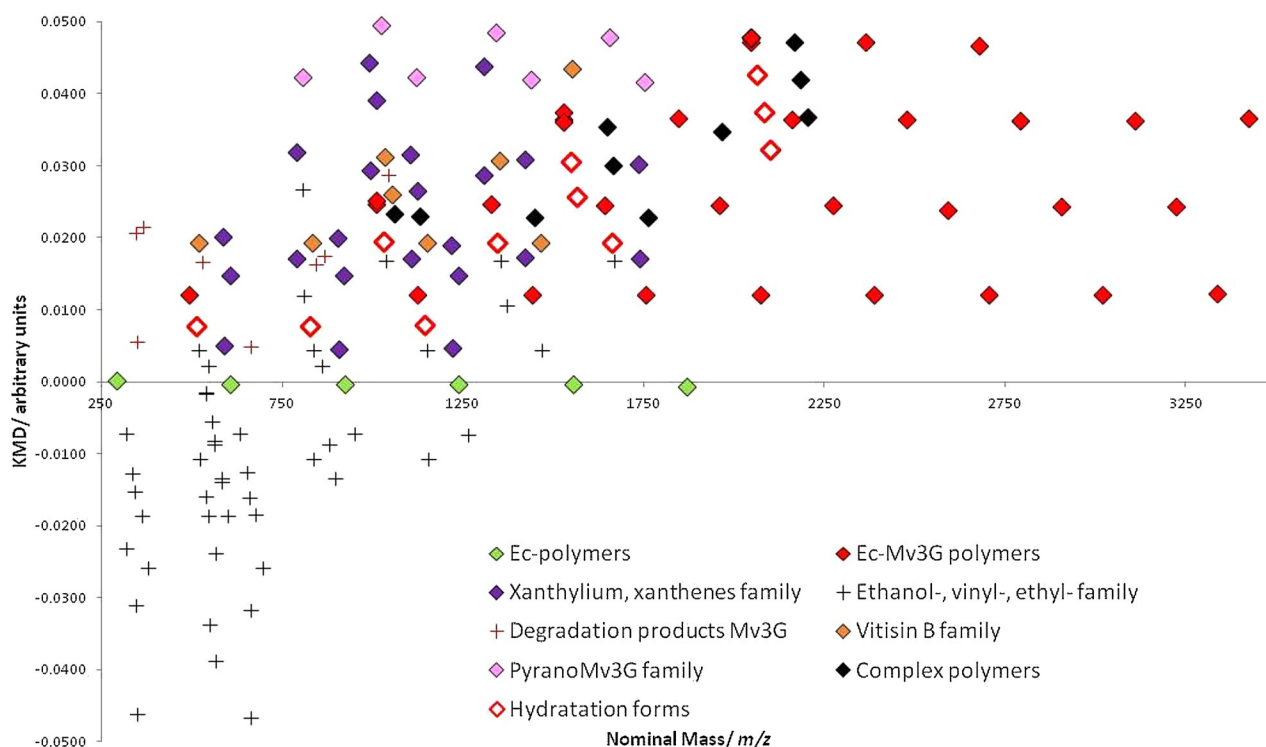


Figure 4. Diagram of Kendrick for all molecules.

some structures, cannot be distinguished from the flavylum form (Tables S1–S7).

The Kendrick representation enabled the detection of several base units, in addition to the initial building blocks (i.e. Ec and Mv3G), each giving rise to a polymer series formed through successive additions of ethyl-Ec and/or ethyl-Mv3G (Figure 4, Tables S2–S7).

These additional building blocks included the known ethyl, vinyl, and ethanol adducts of Ec and Mv3G (Table S2), pyranoMv3G (vitisin B) (Table S3) and Ec-pyranoMv3G (Table S4), but also so far unreported compounds (Tables S1–S7). Among the latter, Mv3G–pyranoMv3G, arising from the cycloaddition of vinyl-Mv3G onto another Mv3G molecule, and its hydrated form were detected (Figure 5, Table S8).

Other new series corresponded to derivatives of xanthene, xanthylum, and hydrated xanthylum forms (Figure 5, Table S8). Two adjacent Ec and/or Mv3G units in ethyl-linked oligomers can cyclize to form xanthenes that oxidize to xanthylum salts, which are in equilibrium with their hydrated form (Table S5). These reactions have been described earlier for condensation products of flavan-3-ols and/or anthocyanins with other aldehydes<sup>[23–24]</sup> or with Ec and acetaldehyde,<sup>[26]</sup> but this is the first report of such molecules arising from the reaction of Ec and/or Mv3G with acetaldehyde.

Each of these building blocks can also combine randomly in the polymerization process, as illustrated by the detection of complex molecules such as vitisin B–ethyl–vitisin B ( $M^{2+}$  detected at  $m/z = 530.1424$ ), vitisin B–ethyl–Ec-pyranoMv3G ( $M^{2+}$  detected at  $m/z = 674.1741$ ), vitisin B–ethyl–Mv3G–pyranoMv3G ( $M^{3+}$  detected at  $m/z = 517.1346$ ), and vitisin B–ethyl–

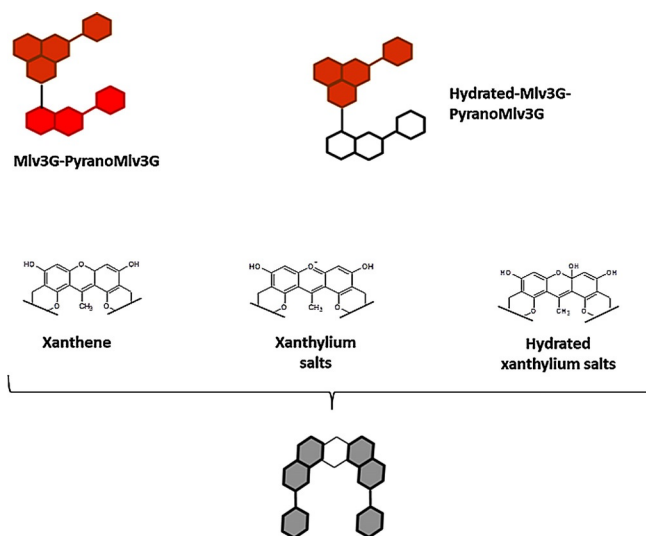


Figure 5. More complex building blocks.

xanthene ( $M^+$  detected at  $m/z = 1131.3138$ ), all of which had not been reported (Table S6).

Other compounds detected on the diagram of Kendrick were degradation products of Mv3G, namely malvone, malvone aglycone, and 3-hydroxyphenylacetyl glucoside,<sup>[27]</sup> that also serve as building blocks because their ethyl-flavonoid derivatives were detected, as well as *cis*- and *trans*-anthocyanone A (8- $\beta$ -D-glucopyranosyl-2,4-dihydroxy-6-oxo-cyclohexa-2,4-dienylacetic acid) (Table S7).

In summary, we demonstrated that, starting from a very simple solution, reaction cascades involving acetaldehyde–flavonoid condensation, dehydration of flavonoid–ethyl–flavonoid units, cycloaddition (yielding pyranoanthocyanins), oxidation (of xanthene to xanthylium), and hydration (of flavylium and xanthylium salts) yield an extremely complex composition, including new compounds. We believe that similar random cascade mechanisms involving many more building blocks and reactions generate the composition of complex real systems such as wines (or other processed food and non-food products). HRMS data analysis associated with a Kendrick mass defect strategy can be successfully applied to describe these systems, detect additional products, building blocks, and reactions, and, using appropriate chemometrics, establish relationships between composition and quality.

## Experimental Section

See the Supporting Information.

## Acknowledgements

We thank the scientific platform of CCIT UB for the technical support. Funding for this work was provided by the Instituto de Salud Carlos III, ISCIII (CIBEROBN), the Quality Group from Generalitat de Catalunya (GC) 2014 SGR 773, and by INRA Departement CEPIA.

## Conflict of Interest

The authors declare no conflict of interest.

**Keywords:** acetaldehyde-mediated condensation • flavonoids • Kendrick mass defect plots • mass spectrometry • polymerization

- [1] S. Quideau, D. Deffieux, C. Douat-Casassus, L. Pouységú, *Angew. Chem. Int. Ed.* **2011**, *50*, 586–621; *Angew. Chem.* **2011**, *123*, 610–646.  
[2] I. Tarascou, J. M. Souquet, J. P. Mazauric, S. Carrillo, S. Coq, F. Canon, H. Fulcrand, V. Cheynier, *Arch. Biochem. Biophys.* **2010**, *501*, 16–22.

- [3] F. Canon, A. R. Milosavljević, G. Van Der Rest, M. Réfrégiers, L. Nahon, P. Sarni-Manchado, V. Cheynier, A. Giuliani, *Angew. Chem. Int. Ed.* **2013**, *52*, 8377–8381; *Angew. Chem.* **2013**, *125*, 8535–8539.  
[4] A. Crozier, I. Jaganath, M. N. Clifford, *Nat. Prod. Rep.* **2009**, *26*, 1001–1043.  
[5] N. Mateus, A. Silva, C. Santo sBuelga, J. C. Rivas-Gonzalo, V. De Freitas, *J. Agric. Food Chem.* **2002**, *50*, 2110–2116.  
[6] V. De Freitas, N. Mateus, *Environ. Chem. Lett.* **2006**, *4*, 175–183.  
[7] V. Cheynier, M. Duenas-Paton, E. Salas, C. Maury, J. M. Souquet, P. Sarni-Manchado, H. Fulcrand, *Am. J. Enol. Vitic.* **2006**, *57*, 298–305.  
[8] J. Wirth, C. Morel-Salmi, J. M. Souquet, H. Fulcrand, V. Cheynier, *Food Chem.* **2010**, *123*, 107–116.  
[9] A. Arapitsas, M. Scholz, U. Vrhovsek, S. Di Blasi, A. Bartolini, D. Masuero, D. Perenzoni, A. Rigo, F. Mattivi, *PLoS One* **2012**, *7*, e37783–e37788.  
[10] M. Duenas, H. Fulcrand, V. Cheynier, *Anal. Chim. Acta* **2006**, *563*, 15–25.  
[11] V. De Freitas, N. Mateus, *Anal. Bioanal. Chem.* **2011**, *401*, 1463–1477.  
[12] V. Cheynier, J. Rigaud, J.-M. Souquet, J.-M. Barillere, M. Moutounet, *Am. J. Enol. Vitic.* **1989**, *40*, 36–42.  
[13] R. F. Simpson, *Vitis* **1982**, *21*, 233–239.  
[14] T. Dier, K. Egele, V. Fossog, R. Hempelmann, A. Dietrich, *Anal. Chem.* **2016**, *88*, 1328–1335.  
[15] A. Vallverdú-Queralt, M. Biler, E. Meudec, C. L. Guernevé, A. Vernhet, J.-P. Mazauric, J.-L. Legras, M. Loonis, P. Trouillas, V. Cheynier, O. Dangles, *Int. J. Mol. Sci.* **2016**, *17*, 1842.  
[16] N.-E. Es-Safi, H. Fulcrand, V. Cheynier, M. Moutounet, *J. Agric. Food Chem.* **1999**, *47*, 2088–2095.  
[17] V. Atanasova, H. Fulcrand, C. Le Guerneve, V. Cheynier, M. Moutounet, *Tetrahedron Lett.* **2002**, *43*, 6151–6153.  
[18] L. Cruz, R. F. Bras, N. Teixeira, A. Fernandes, N. Mateus, J. Ramos, J. Rodriguez-Borges, V. De Freitas, *J. Agric. Food Chem.* **2009**, *57*, 10341–10348.  
[19] H. Fulcrand, P. J. Cameira dos Santos, P. Sarni-Manchado, V. Cheynier, J. J. Favre-Bonvin, *Chem. Soc. Perkin. Trans.* **1996**, *1*, 735–739.  
[20] H. Fulcrand, C. Benabdeljalil, J. Rigaud, V. Cheynier, M. Moutounet, *Phytochemistry* **1998**, *7*, 1401–1407.  
[21] J. Bakker, P. Bridle, T. Honda, H. Kuwano, N. Saito, N. Terahara, C. Timberlake, *Phytochemistry* **1997**, *7*, 1375–1382.  
[22] L. Cruz, N. Teixeira, A. M. Silva, N. Mateus, J. Borges, V. de Freitas, *J. Agric. Food Chem.* **2008**, *56*, 10980–10987.  
[23] N. E. Es-Safi, V. Cheynier, M. Moutounet, *J. Agric. Food Chem.* **2000**, *48*, 5946–5954.  
[24] N. E. Es-Safi, C. Le Guernevé, V. Cheynier, M. Moutounet, *J. Agric. Food Chem.* **2000**, *48*, 4233–4240.  
[25] N. E. Es-Safi, V. Cheynier, M. Moutounet, *J. Agric. Food Chem.* **2002**, *25*, 5586–5595.  
[26] A. Vallverdú-Queralt, E. Meudec, M. Eder, R. M. Lamuela-Raventos, N. Sommerer, V. Cheynier, *Food Chem.* **2017**, *227*, 255–263.  
[27] A. Vallverdú-Queralt, E. Meudec, N. Ferreira, N. Sommerer, O. Dangles, V. Cheynier, C. Le Guerneve, *Food Chem.* **2016**, *199*, 902–910.

Received: March 2, 2017

Version of record online May 15, 2017